Compact red–green–blue beam illuminator and expander

Revital Shechter, Nandor Bokor, Yaakov Amitai, and Asher A. Friesem

A compact multicolor beam illuminator and a compact multicolor beam expander are presented. The illuminator performs the dual task of demultiplexing a narrow red–green–blue (RGB) input beam into three separate beams, each of a different color, and expanding them to yield three separate magnified plane waves. The beam expander expands a narrow RGB input beam into a single magnified RGB plane wave. The design and recording procedures, along with experimental results for a beam illuminator and a beam expander with a magnification of ~3, are presented. © 2002 Optical Society of America

OCIS codes: 050.1970, 050.1950, 050.7330, 090.4220, 999.9999.

1. Introduction

Beam illuminators and expanders magnify a narrow collimated beam into a beam of larger diameter. They have been implemented in a variety of applications, such as lasers,[1–3] fiber optics,[4] medical diagnostics,[5] holography,[6,7] x-ray optics,[8] and the space industry.[9] In general, beam expanders are composed of two lenses or mirrors with a common focal point in a telescopic configuration. When a compact configuration is needed, it is advantageous to use a Galilean telescope (composed of a negative lens and a positive lens), which has a smaller length than a Keplerian telescope (composed of two positive lenses) with the same magnification and pupil sizes. With monochromatic illumination, the overall size can be further reduced by holographic lenses and planar optics configurations.[10–12] In this case, light propagates between the lenses inside a substrate by total internal reflection.

In this paper, we extend the planar configuration to include red–green–blue (RGB) illumination, which can be useful for display and projection applications. Specifically, we present two different configurations. The first one is a compact planar beam illuminator that separates the RGB components of an incident beam into three monochromatic beams and then expands them in three different directions. The second one is a compact beam expander that expands an incident white-light beam to a white-light beam of larger diameter. The beam illuminator is composed of four diffractive optical elements (DOEs) that are recorded on the same substrate. One of the DOEs, composed of three superimposed diffractive optical lenses, demultiplexes a narrow multicolor (RGB) plane wave into three diverging spherical waves that travel at sufficiently high diffraction angles so that they are trapped inside the substrate by total internal reflection. Each of these three waves propagates in a different direction in the substrate, impinges on a second diffractive lens, and then emerges from the substrate as a magnified quasi-monochromatic plane wave. The beam expander, on the other hand, consists of two DOEs, both composed of three superimposed diffractive optical lenses. The first DOE transforms all three components of an incoming RGB plane wave into diverging spherical waves that are trapped by total internal reflection inside the substrate and propagate toward the second DOE. The three monochromatic beams are coupled out by the second DOE and emerge from the substrate as a single expanded white-light plane wave.

2. Basic Configuration and Design Considerations

We begin with the basic configuration of a monochromatic beam expander by using diffractive lenses, shown in Fig. 1. Figure 1(a) shows an unfolded configuration with two diffractive lenses in the free space. A narrow, collimated beam with a diameter D_1 is diffracted by negative lens H_1, which has a focal length f_1, into an off-axis expanding spherical wave. The spherical wave is then diffracted by positive lens H_2, which has a focal length f_2, to form a collimated beam with a diameter D_2. The overall magnification

The authors are with the Department of Physics of Complex Systems, Weizmann Institute of Science, 76100 Rehovot, Israel. When this research was performed, N. Bokor was on leave from the Department of Physics, Budapest University of Technology and Economics, Budafoki ut 8., 1111 Budapest, Hungary. R. Shechter's e-mail address is ferevita@wisemail.weizmann.ac.il.

Received 12 February 2001; revised manuscript received 25 July 2001.

0003-6935/02/071229-07$15.00/0

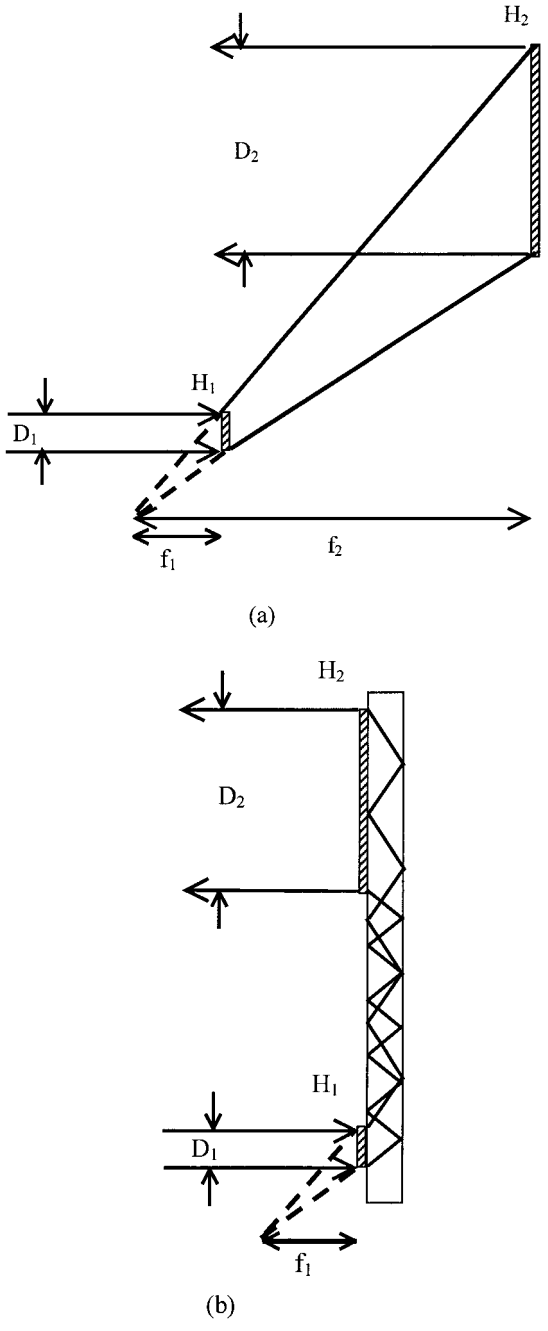

Fig. 1. Basic configuration of a monochromatic diffractive beam expander: (a) unfolded configuration, (b) folded, planar configuration. H_1 and H_2 are two diffractive lenses with focal lengths f_1 and f_2, respectively. D_1 and D_2 are the input and the output beam diameters, respectively. In the folded configuration of (b), light propagates between the two diffractive lenses inside the substrate by total internal reflection.

of the beam expander is $M = D_2/D_1 = f_2/f_1$. Figure 1(b) shows the corresponding folded, compact planar configuration. Here the two diffractive lenses are recorded on the same substrate, and light propagates from one lens to the other inside the substrate by total internal reflection.

The planar configuration with monochromatic illumination can be extended to one with RGB illumination to form either a beam illuminator or a beam expander, as shown in Fig. 2. Figure 2(a) shows a planar configuration for a RGB beam illuminator. Here both wavelength demultiplexing and beam expansion are achieved with input element H_{1RGB}, which is composed of three superimposed DOEs. The three output lenses, H_{2R}, H_{2G}, and H_{2B}, are laterally displaced. Each of these three lenses is a DOE that is optimized for a different wavelength. Figure 2(b) shows the planar configuration for the RGB beam expander, which is a multicolor version of the monochromatic expander shown in Fig. 1(b). Here both input element H_{1RGB} and output element H_{2RGB} are composed of three superimposed DOEs.

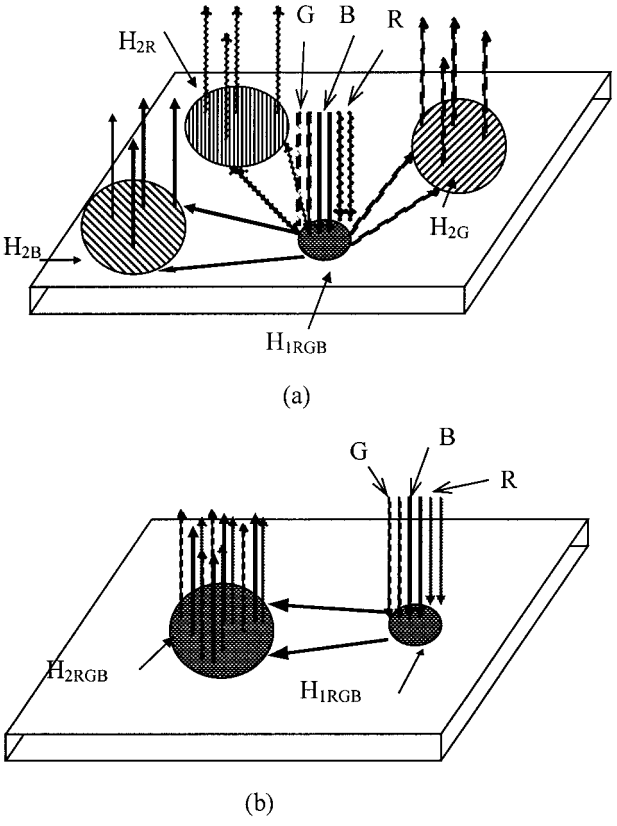

Fig. 2. Planar configuration of compact RGB beam (a) illuminator, (b) expander. In (a) composite diffractive lens H_{1RGB} expands and demultiplexes the incoming RGB light and sends the three components to three different diffractive lenses, H_{2R}, H_{2G}, and H_{2B}, from which they emerge as magnified monochromatic plane waves. In (b) composite diffractive lens H_{1RGB} expands the incoming RGB light and sends it to H_{2RGB}, another composite diffractive lens, from which a magnified RGB plane waves emerges.

A detailed geometry of a planar diffractive lens and the associated light rays for each planar diffractive element is presented in Fig. 3. As shown, l is the thickness of the glass substrate, t is the thickness of the recording medium, f is the focal length of the lens, x is the coordinate along the lens corresponding to the ray with diffraction angle θ from the virtual focus, and x' is the coordinate along the lens corresponding to the ray with diffraction angle θ'. The diffraction

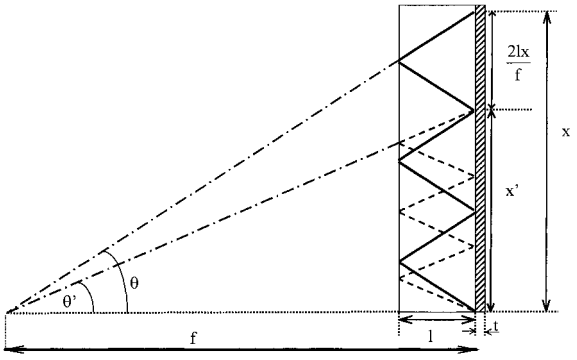

Fig. 3. Geometry of a planar diffractive lens and associated rays: f is the focal length of the lens, l is the thickness of the substrate, t is the thickness of the recording material, and x and x' are lateral coordinates along the lens, corresponding to light rays of angles θ and θ', respectively.

angles are such that even the smallest angle θ' is larger than the critical angle needed for total internal reflection, which means that

$$\theta' > \sin^{-1}(1/n), \tag{1}$$

where n is the refractive index of the substrate. To minimize any undesired interactions between the trapped rays and the DOEs, we have to impose certain design considerations. These include proper choice of the thickness and the phase modulation of the recording material, the thickness of the substrate, and the aperture size of the DOEs. As shown in Fig. 3, there are multiple reflections inside the substrate, so each ray could be coupled out by the second diffractive element at several locations that are separated by $2lx/f$, leading to undesired noise and ghost images. To minimize these undesired diffractions, we use thick recording materials, so that efficient diffraction occurs only around the Bragg angle, which for our specific coupling-out diffractive lens differs at each location on the lens. Specifically, it is necessary to ensure that the angle θ of the ray that is internally reflected at x' differs sufficiently from the Bragg angle θ' at this point, so that only the desired ray with the angle θ' will be diffracted outward. In this way, a sufficiently low cross talk will be achieved between rays having angles θ and θ' at the location x'.

We calculated the diffraction efficiency as a function of the lateral coordinates of the planar diffractive lenses for all the rays by using Kogelnik's coupled-wave theory for thick diffractive gratings.[13] The calculations were performed for three wavelengths: $\lambda_1 = 488$ nm, $\lambda_2 = 514.5$ nm, and $\lambda_3 = 647$ nm, with the parameters $n = 1.51$, $t = 20$ μm, $l = 1.6$ mm, and $f = 33$ mm. Some representative results for a diffractive lens that was designed to operate with illumination wavelength of $\lambda_3 = 647$ nm are shown in Figs. 4 and 5. All the calculated results presented are for TE illumination. Similar results can be obtained for TM illumination when Kogelnik's theory is used.[13] (We justify our choice of TE illumination below when we talk about the composite DOE

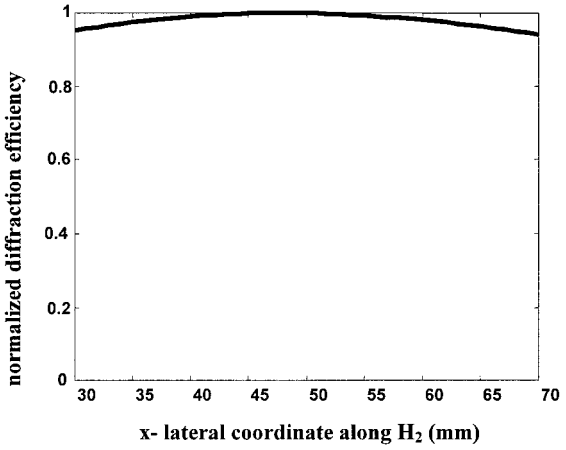

Fig. 4. Calculated diffraction efficiency as a function of the lateral coordinate for a planar diffractive lens designed to operate with $\lambda = 647$ nm.

H_{1RGB}.) Figure 4 shows the desired Bragg diffraction efficiency, for the rays impinge on the "proper places," as a function of lateral coordinate x along DOE H_2. Figure 5 shows the undesired diffracted light efficiency resulting from non-Bragg diffraction as a function of x. As can be seen, there is a section between $x \sim 35$ and $x \sim 60$ mm where the desired diffraction efficiency is greater than 95% and the cross talk is less than -17 dB (or 2%). Thus, despite the multiple reflections inside the substrate, significant diffractions occur at only the desired locations. Similar results were obtained for the diffractive lenses that were designed to operate with the wavelengths λ_1 and λ_2.

For our specific configuration design it is necessary to ensure during the design procedure that 1, H_2 is within 35 to 60 mm; 2, the off-axis angles for all the trapped rays are greater than 42° (the critical angle to achieve total internal reflection for material with $n = 1.51$); 3, the distance between the centers of H_1 and H_2 is such that the internally propagating wave

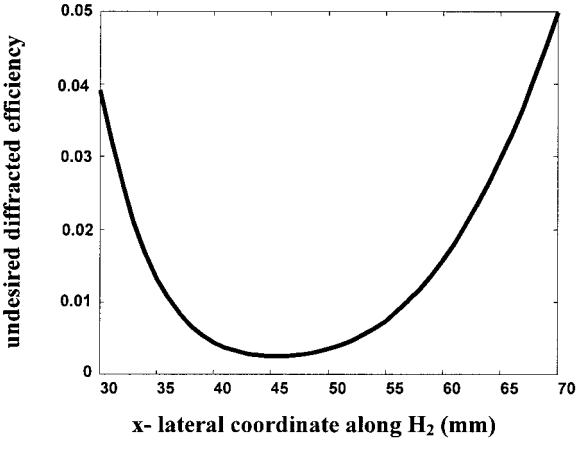

Fig. 5. Calculated undesired diffraction efficiency (cross talk) as a function of the lateral coordinate for a planar diffractive lens designed to operate with $\lambda = 647$ nm.

undergoes an even number of reflections [this condition can be satisfied if the difference between the focal lengths, $f_2 - f_1$, is an even multiple of the overall thickness $(l + t)$], and (4) the magnification is at least 3. The resulting design parameters for the sizes of H_1 and H_2 are the following: The limits of H_2 are between 39.3 and 57.2 mm and hence $D_2 = 57.2 - 39.3 = 17.9$ mm, and the limits of H_1 are between 12.6 and 18.4 mm and hence $D_1 = 5.8$ mm. Therefore the magnification of the optical system is $M = D_2/D_1 = 3.1$. It should be noted that for all the coupling-out lenses the zero diffraction order remains trapped inside the plate by total internal reflection and can be absorbed at the edge of the substrate.

Finally, because H_{1RGB} is composed of three sub-DOEs whose task, in the case of the beam illuminator, is also to demultiplex three different wavelengths, it is necessary to ensure that each sub-DOE will diffract only its respective wavelength and will be actually transparent for the other two wavelengths; that is, the chromatic cross talk, which is set by the diffraction of beams whose wavelengths differ from the desired wavelength, should be minimized and the diffraction efficiency of the desired beams should be as high as possible for all three sub-DOEs. To ensure high diffraction efficiency at a certain lateral coordinate x for a given sub-DOE on H_{1RGB} and for TE illumination, the relation[13]

$$\frac{2\Delta n_i t}{\lambda_i \sqrt{\cos\,\theta}} = 2m - 1 \tag{2}$$

should be satisfied, where $\Delta n_{i\mathrm{TE}}$ is the refractive-index modulation, λ_i is the wavelength in free space, θ is the desired off-axis angle at x (see Fig. 3), and m is an integer number. Hence, for a given t, θ, m and λ_i, the necessary refractive-index modulation to achieve high diffraction efficiency is given by

$$\Delta n_{i\mathrm{TE}} = \frac{(2m - 1)\lambda_i \sqrt{\cos\,\theta}}{2t}. \tag{3}$$

For TM illumination the corresponding necessary index modulation is[13]

$$\Delta n_{i\mathrm{TM}} = \frac{\Delta n_{i\mathrm{TE}}}{\cos\,\theta}. \tag{4}$$

For $t = 20$ μm, $m = 1$, and $\theta = 55°$ (this corresponds to the center of H_{1RGB} in our design) we get the following values for the necessary refractive-index modulation:

$$\begin{aligned}
&\text{for } \lambda_i = 488 \text{ nm}, \Delta n_{i\mathrm{TE}} = 0.0092, \Delta n_{i\mathrm{TM}} = 0.016;\\
&\text{for } \lambda_i = 514.5 \text{ nm}, \Delta n_{i\mathrm{TE}} = 0.0097, \Delta n_{i\mathrm{TM}} = 0.017;\\
&\text{for } \lambda_i = 647 \text{ nm}, \Delta n_{i\mathrm{TE}} = 0.0123, \Delta n_{i\mathrm{TM}} = 0.0214.
\end{aligned} \tag{5}$$

The number of sub-DOEs that can be multiplexed on the same location is determined by the refractive-index saturation of the recording material. Specifically, N different sub-DOEs can be multiplexed on the same photosensitive material with high efficiencies, negligible absorption, and with no index saturation, if the condition[14]

$$\sum_{i=1}^{N} \Delta n_i \le \Delta n_{\max} \tag{6}$$

is satisfied, where N is the desired number of sub-DOEs (in our case $N = 3$). For the DuPont photopolymer that we used, $\Delta n_{\max} \approx 0.05$–$0.06$, so the condition given in relation (6) can be satisfied for only TE illumination. Accordingly, throughout the experiments we chose to optimize the recording process of both H_{1RGB} and H_{2RGB} for a readout light having TE polarization. In the reconstruction process, TE-polarized RGB beams were used for the beam illuminator, and white unpolarized light was used for the beam expander. Because the unpolarized light contains TM components too, it is expected that the diffraction efficiency is lower than that for pure TE illumination. We can calculate the degradation in diffraction efficiency for a case in which H_{1RGB} is recorded for a readout light having TE polarization with optimal $\Delta n_{i\mathrm{TE}}$ index modulations and then reconstructed with TM polarization. For the center of H_{1RGB} ($\theta = 55°$) the diffraction efficiency of the TM light is $\eta_{\mathrm{TM}} = \sin^2[(\pi/2)\cos\,\theta] = 0.61$. Hence for unpolarized illumination it is expected that the overall diffraction efficiency will be ~80%. In Section 4 it is demonstrated that satisfactory experimental results were obtained with unpolarized readout illumination for the beam expander. It is important to note that, when a different recording material with higher $\Delta n_{\max}$ is used, an efficient H_{1RGB} for any desired polarization can be designed and recorded in a relatively straightforward way. Furthermore, an efficient H_{1RGB} for unpolarized readout illumination can be designed if trade-off values for Δn_1, Δn_2, and Δn_3 that give optimal efficiency for all possible polarizations are found.

The other important requirement for H_{1RGB} is its wavelength selectivity. It has been shown[15] that the efficiency of a volume DOE with TE readout illumination drops to zero when the wavelength deviation from Bragg condition satisfies the following approximate relation:

$$\Delta\lambda_i \approx \frac{\sqrt{3}}{4nt} \frac{{\lambda_i}^2}{\sin(\theta/2)\tan(\theta/2)}. \tag{7}$$

Using the parameters given in Eqs. (5), we find that the approximate $\Delta\lambda$ values at the center of H_{1RGB} are

$$\begin{aligned}
&\text{for } \lambda_1 = 488 \text{ nm}, \Delta\lambda = 14 \text{ nm};\\
&\text{for } \lambda_1 = 514.5 \text{ nm}, \Delta\lambda = 16 \text{ nm};\\
&\text{for } \lambda_1 = 647 \text{ nm}, \Delta\lambda = 25 \text{ nm}.
\end{aligned} \tag{8}$$

These results imply that there is sufficient wavelength separation among λ_1, λ_2, and λ_3 to ensure low chromatic cross talk. Using Kogelnik's theory, we calculated the entire spectral response of the three sub-DOEs at the center of H_{1RGB}. The results are

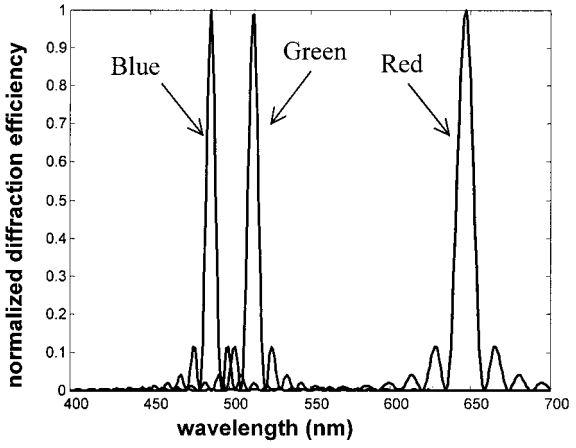

Fig. 6. Calculated diffraction efficiency of H_{1RGB} as a function of wavelength.

presented in Fig. 6. As can be seen, the sub-DOE designed for the red wavelength is completely transparent to the other two wavelengths, whereas there is approximately a −20-dB (~1%) chromatic cross talk between the two sub-DOEs designed for the blue and the green wavelengths. We also calculated the chromatic cross talk between any two wavelengths as a function of location over the entire area of H_{1RGB}. The results are shown in Fig. 7. As expected, the chromatic cross talk is greater when the two wavelengths are closer to each other, but even in the worst case (the cross talk between 488 and 514.5 nm) it is less than −18 dB (1.6%) over the entire area of H_{1RGB}.

3. Experimental Procedure and Results

The recording setup for a representative DOE is shown in Fig. 8. The DOEs were holographically recorded, separately for each wavelength, with a perpendicularly incident plane wave and an off-axis spherical wave for each recording. To ensure that during reconstruction the diffracted light would be trapped within the substrate, the recording beams were passed through a prism attached to the substrate with an index-matching fluid. As can be seen in Fig. 8, the prism and the photopolymer were positioned so that the focal point of the spherical wave coincided with the surface of the prism. This is necessary to minimize aberrations introduced in the spherical wave by the prism surface. All the DOEs were recorded on the same glass plate substrate, which was coated with polychromatic sensitive DuPont photopolymer film. The photopolymer had sufficient thickness (t = 20 μm) and index modulation ($\Delta n_{max} \approx 0.05–0.06$) to obtain volume Bragg gratings with high diffraction efficiencies and sufficient wavelength and angular selectivity at each location on the DOEs. For the beam illuminator the substrate was rotated by 90° between exposures with different wavelengths. The rotation was done around the center of H_{1RGB}, so that the three sub-DOEs of H_{1RGB} were superimposed on the same location. For the beam expander, the three sub-DOEs of H_{1RGB} and H_{2RGB} were independently recorded, each with three different wavelengths, with no rotation or lateral movement between individual recordings of the same lens. We recorded the DOEs sequentially (because we used the same Ar laser for the 488- and the 514.5-nm recordings), but it is important to note that exposing the three sub-DOEs simultaneously and optimizing the intensity of each wavelength would probably yield better results.[16]

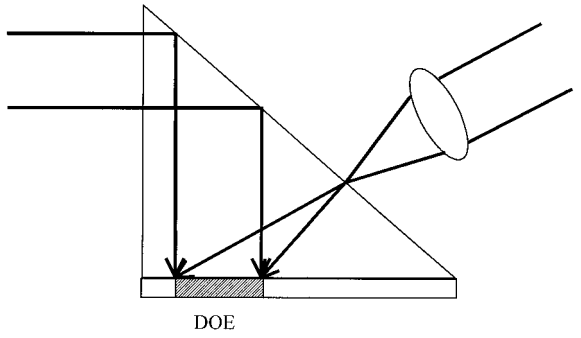

Fig. 8. Recording setup for one DOE. The interference pattern of a perpendicularly incident plane wave and an obliquely incident spherical wave is recorded on photopolymer. The prism is needed to ensure a large enough oblique angle for the spherical wave. The prism and the photopolymer are positioned so that the focal point of the spherical wave coincides with the surface of the prism in order to minimize aberrations introduced in the spherical wave by the prism surface.

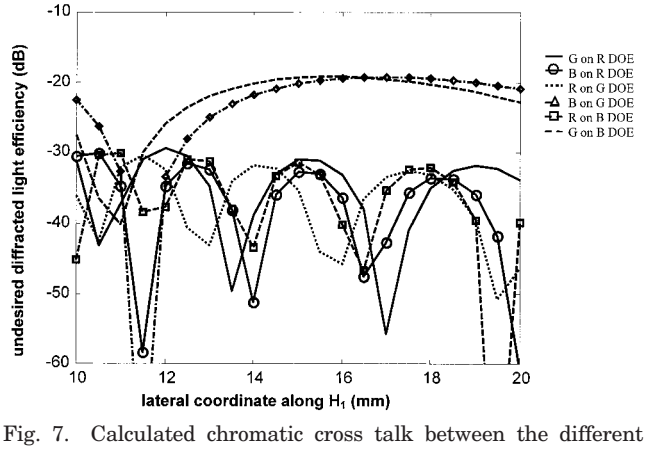

Fig. 7. Calculated chromatic cross talk between the different wavelengths at H_{1RGB} as a function of the lateral coordinate.

The experimental results are presented in Figs. 9–11. Figure 9 shows a scan of the spectral response of a representative H_{1RGB}, made with white-light illumination. The experimental graph of Fig. 9 corresponds to the calculated results of Fig. 6. As can be seen, the experimental spectral bandwidths are broader than the calculated bandwidths. This broadening can be explained by imperfections during the recording process and also by the fact that the experimental results represent an average value over the entire lens, rather than the intensity on the central spot.

We also measured the chromatic cross talk be-

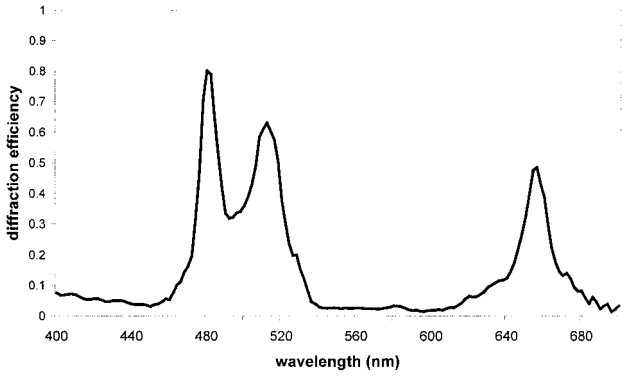

Fig. 9. Experimental diffraction efficiency for a representative H_{1RGB} as a function of wavelength.

tween the sub-DOEs of H_{1RGB}. We did this by sequentially illuminating H_{1RGB} with a beam of one wavelength and measuring the percentage of the light that was diffracted toward the wrong DOEs (which were designed for the other two wavelengths). The results are summarized in Table 1. As expected, the chromatic cross talk was below 35 dB between the red and either of the other two wavelengths. On the other hand, higher cross-talk values (~16.5 dB) were measured between the sub-DOEs designed for 514.5 and 488 nm.

Figure 10 shows a photograph of the light distribution of the input and the output beams of the RGB beam illuminator. As can be seen, the input RGB beam at the center is relatively small in diameter, and the separate output beams, each of a different wavelength, are larger. In this experiment, the input beam was formed by three collimated beams of $\lambda_1 = 488$ nm, $\lambda_2 = 514.5$ nm, and $\lambda_3 = 647$ nm, emerging from an Ar and a Kr laser. The throughput light efficiency of each wavelength was approximately 30–40%, indicating average diffraction efficiency of 55–65% for each separate DOE. There was some undesired scattering of light in the path between the input and the output DOEs. This is due to the noise of the photopolymer recording material,

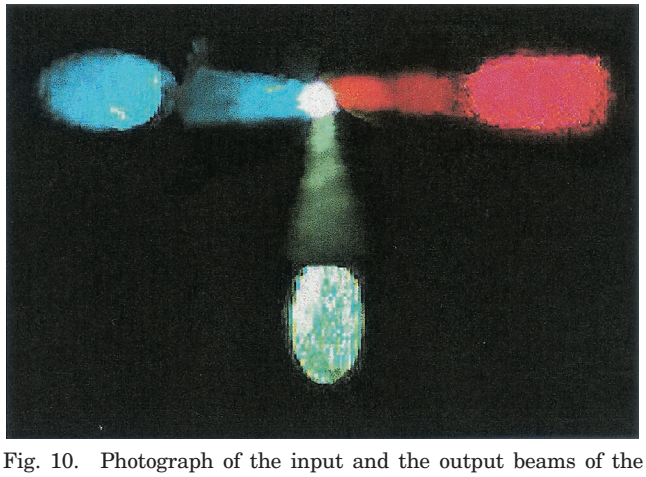

Fig. 10. Photograph of the input and the output beams of the compact RGB beam illuminator.

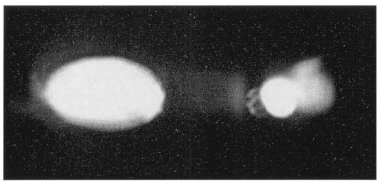

(a)

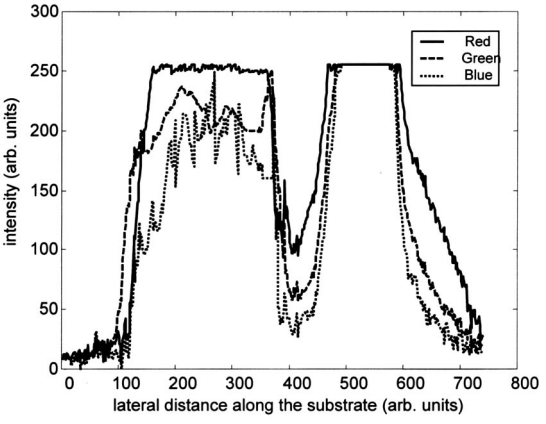

(b)

Fig. 11. Input and output beams of the compact RGB beam expander: (a) photograph of the light distribution, (b) intensity scans for the RGB wavelengths.

and this disturbance can be reduced if the photopolymer material along the path is removed. Figure 11 illustrates the light distribution of the input and the output beams of the RGB beam expander. Figure 11(a) shows a photograph of the input and the output beams. Here the input illumination was a collimated, unpolarized white-light beam. The input beam in Fig. 11(a) is slightly smeared because of a secondary image that came from an undesired reflection in the system. Figure 11(b) shows the corresponding intensity scans for each of the three wavelengths. These results indicate a uniform response over the input DOE, whereas the ratio between the colors at the output needs optimization. The overall throughput light efficiency of this expander was approximately 40–50%, indicating an average diffraction efficiency of 65–70% for each separate sub-DOE. Thus, although the design was done for TE polarization and in this case the DOEs

Table 1. Measured Chromatic Cross Talk of H_{1RGB}

	λ (nm)		
Beam Direction	488 (dB)	514.5 (dB)	647 (dB)
To red	< −35	< −35	—
To green	−16.4	—	< −35
To blue	—	−16.8	< −35

were reconstructed with unpolarized light, the performance is still satisfactory.

4. Concluding Remarks

We have presented compact, planar beam illuminator and beam expander configurations that are capable of handling multicolor RGB illumination simultaneously. The results of diffraction efficiency and cross talk can be improved if the recording process is optimized for the different wavelengths. Satisfactory diffraction efficiencies along with negligible cross-talk values were achieved for both configurations. The arrangements presented here can be useful for numerous display and projection applications.

References

1. M. Chapman and N. R. Heckenberg, "Use of a beam expanding telescope in grating-tuned waveguide CO_2 laser," Int. J. Infrared Millim. Waves **8,** 783–791 (1987).
2. M. Chien, U. Koren, T. L. Koch, B. I. Miller, M. Oron, M. G. Young, and J. L. Demiguel, "Short-cavity distributed Bragg reflector laser with an integrated tapered output waveguide," IEEE Photonics Technol. Lett. **3,** 418–420 (1991).
3. M. Takahashi and T. Ohntoshi, "Finite-difference time-domain analysis of laser diodes integrated with tapered beam-expanders," IEEE Photonics Technol. Lett. **11,** 524–526 (1999).
4. F. Martinez, G. Wylangowski, C. D. Hussy, and F. P. Payne, "Design and implementation considerations for a practical self-aligned single-mode fibre-horn beam expander," presented at the 13th European Conference on Optical Communication, Helsink, Finland, 13–17 September 1987, Vol. 1 of Technical Digest, 379–382.
5. S. K. Gayen, M. E. Zevallos, B. B. Das, and R. R. Alfano, "Time-sliced, two-dimensional, near-infrared imaging of normal and malignant human breast tissues," in *Conference on Lasers and Electro-Optics* (*CLEO/U.S.*), Vol. 6 of 1998 OSA Technical Digest Series (Optical Society of America, Washington, D.C., 1998), pp. 230–231.
6. Wu Jiang, D. L. Shealy, and K. M. Baker, "Physical optics analysis of the performance of a holographic projection system," in *Diffractive and Holographic Optics Technology II*, I. Cindrich and S. H. Lee, eds., Proc. SPIE **2404,** 227–234 (1995).
7. P. Hariharan, "Beam expander for making large rainbow holograms," Appl. Opt. **26,** 1815–1818 (1987).
8. F. E. Christensen, A. Horntrup, P. Frederiksen, C. Nilsson, P. Grundsoe, P. Orup, E. Jacobsen, H. W. Schnopper, R. Lewis, and C. Hall, "A beam expander facility for studying x-ray optics," Rev. Sci. Instrum. **63,** 1168–1171 (1992).
9. M. S. Scholl and G. N. Lawrence, "Diffraction modeling of a space relay experiment," Opt. Eng. **29,** 271–278 (1990).
10. R. K. Kustuk, M. Kato, and Y. T. Huang, "Substrate mode holograms for optical interconnects," in *Optical Computing*, Vol. 9 of 1989 OSA Technical Digest Series (Optical Society of America, Washington, D.C., 1989), pp. 168–171.
11. A. A. Friesem and Y. Amitai, "Planar diffractive elements for compact optics," in *Trends in Optics*, A. Consortini, ed. (Academic, San Diego, 1996), pp. 125–144.
12. I. Shariv, Y. Amitai, and A. A. Friesem, "Compact holographic beam expander," Opt. Lett. **18,** 1268–1270 (1993).
13. H. Kogelnik, "Coupled wave theory for thick holograms and their applications," Bell Syst. Tech. J. **48,** 2909–2947 (1969).
14. F. Lin, E. M. Strzelecki, and T. Jannson, "Optical multiplanar VLSI interconnects based on multiplexed waveguide holograms," Appl. Opt. **29,** 1126–1133 (1990).
15. L. Solymar and D. J. Cooke, *Volume Holography and Volume Gratings* (Academic, London, 1981), Chap. 4.
16. S. H. Lin, K. H. Su, W.-Z. Chen, and W. T. Whang, "Exposure schedule for multiplexing holograms in photopolymer," in *Photorefractive Fiber and Crystal Devices: Materials, Optical Properties, and Applications V*, F. T. Yu and S. Yin, eds., Proc. SPIE **3801,** 100–106 (1999).